

Improving the Transmitting Loop Antenna: An Applied Model to Satellite Technology

Emetere Moses E¹, Uno E. Uno², Onyechekwa Lawrence¹ and Sanni E. Samuel³

*1*Department of Physics, Covenant University, Ota, Nigeria

*2*Department of Physics, Federal University of Technology, Minna, Nigeria

*3*Department of Chemical Engineering, Covenant University, Ota, Nigeria

moses.emetere@covenantuniversity.edu.ng

Abstract

The ab-initio Maxwell's equation was introduced using the Schrödinger equation and the Legendre polynomial. The efficiency, bandwidth and size of the transmitting loop was resolved theoretically to enhance the transmission of successive pulses of radio waves to illuminate objects. The radiation characteristics the resonant loop pattern of the loop antenna have been improved via the introduction of the ground plane. However, the perfect results have not been obtained. Further simulation of a dummy experimentation revealed the possibility of a high efficiency in the transmitting loop antenna via the introduction of angular loop displacement along a well defined axis. The results were confirmed experimentally. When the angular loop displacement is $\pi/2$, we expect to see an improved uplink task under either bad or good weather.

Keywords: *transmitting loop antenna, Maxwell's equation, size, Schrödinger equation, Scanning Multichannel Microwave Radiometer*

1. Introduction

One of the advantages of the transmitting loop antennas is its ability to function perfectly within the limits of a full sized antenna limited by space. Before now, it is believed that small transmitting loop antennas sacrifice higher or larger bandwidth for small size and efficiency. The more efficient they are, the narrower the frequency range in which they can operate. In other words, the greatest achievement has been to attain two options out of the three i.e. small size (in terms of wavelength), efficiency and broadband. Small loop antennas are often referred to as magnetic antennas because they mostly respond to the magnetic component of an electromagnetic wave and transmit a large magnetic component in the extreme near field ($<1/10$ wavelength distance). In the far field (>1 wavelength distance) the radio frequency (RF) from a small loop is the same as that from any other antenna being composed of both electric and magnetic fields [1, 3]. At distances between about $1/10$ and 1 wavelength it responds more to the electric field than the magnetic field. Hence, this paper proposes the adoption of the principles of loop antennas in Scanning Multichannel Microwave Radiometer (SMMR) to account for or curb losses due to the motion of the SMMR antenna over a target region (see Figure 1). This feat is achieved when successive pulses of radio waves are transmitted to "illuminate" a target scene with higher frequency within specified bandwidth. The application of antenna technology in mobile communication has been reported by Rasool *et al.* [8]. The system design is an array of antenna with half a wave and a loop antenna. The proposed array of antenna has the capacity of improving the quality of service delivered from wireless systems via steered radiation streaming in the direction of a desired signal source and to also receive signals at constant level amidst the variation in the angle of elevation and the mobile satellite station. A field strength meter (FSM) was used in conducting the experiment at distances within the range of 3 – 33 cm. Results

from the simulation as compared to the experiment showed that the array of systems received signals of 4.3dB more from the moving satellite but in the direction vertical to the antenna system.

Schreiner *et al.* [7] investigated the noise level and receiver stability of Global Positioning Systems (GPS) using data collected from two independently developed Radio Occultation (RO) instruments flying in orbit on the FORMOSAT-3/COSMIC (F3C) and Metop/GRAS (GNSS Receiver for Atmospheric Sounding) missions. The two data sources were investigated with the former post-processed at a frequency of 50 Hz using single difference excess atmospheric phase algorithm and the latter was down-sampled between 50 and 1000 Hz. The results of the standard deviations of the processed signals over a six month period and at an altitude of 60 -80 km showed that F3C has higher bending angle relative to Metop/G due to climatology. Hearn [8] carried out an investigation that involves the formation of Ionospheric Observation Nanosat to investigate the flight requirements for multiple spacecraft missions. The setup includes a communication subsystem for the mission comprising an uplink, a downlink and a satellite-to-satellite crosslink. A linearly polarized resonant loop antenna mounted above the bottom surface of the spacecraft was selected to serve as a satellite uplink receiver antenna. The resonant loop was chosen to satisfy the physical requirements of the spacecraft. A full-scale prototype was fabricated to measure frequency dependent characteristics of the antenna. A gamma match and a quarter-wave sleeve balun transformer were integrated to the system to minimize the power reflected at the antenna input section and so as to isolate the antenna from the feed line. The findings show that the uplink antenna demonstrated sufficient performance. However, it was concluded that in order to achieve the final bandwidth of less than one percent (i.e. 0.01), there must be some additional tuning (increased frequency) owing to other subsystems that are integrated into the final flight-ready prototype. In Wübbena *et al.* [10], several GNSS receivers have been tested with satellite antenna. The gain and gain differences were reported to be significantly different from those of regular GPS receivers (antenna). Although, the signal fed to the receiver may differ from the expected output in relation to the signal processing within the receiver. The paper reveals that the processed signal was finally damped at 22 dB which was adequate for proper receiver operation but when the tracking loop and navigation modes of the receiver were enabled, such that the initial noise level of 22 dB was fed in with power supplied from a voltage source of 9.5 V, the tracking of the tested receivers were seen to differ slightly. In this paper, the standing wave function as it applies to the Schrödinger equation was discussed analytically. Vital parameters which determine the efficiency of transmitting loop antennas were obtained for further industrial research. The resonance frequencies with respect to the theorized model (Legendre polynomial) were worked out.

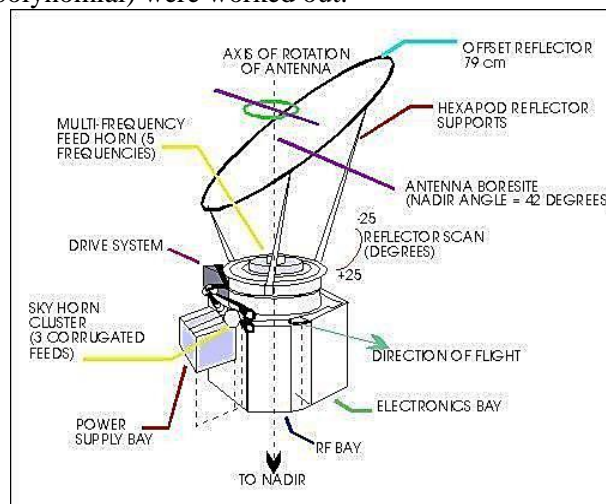


Figure 1. Loop Application in Scanning Multichannel Microwave Radiometer

2. Theoretical Background

The Euler-Lagrange equation (1-4) associated to the function $S = f(T, S, \theta, A)$ gives rise to the following system of equations (1-3)

$$T_{tt} - \Delta T + \left[\frac{\hbar^2}{2m} |\nabla S - eA|^2 + |S_t + V_o e|^2 - \left(|S_t - E_o e \left(\frac{a^2}{x} - x \right)|^2 - |S_t| \right) + 2E_o V_o e^2 + V \right] T = 0 \quad (1)$$

$$\frac{\partial}{\partial t} [(S_t + V_o e) T^2] - \frac{\partial}{\partial t} \left[\left(S_t + E_o e \left(\frac{a^2}{x} - x \right) \right) T^2 \right] - \frac{1}{2} \frac{\partial S_t}{\partial t} + \text{div}[(\nabla S - eA) T^2] = 0 \quad (2)$$

$$E_o e \left(\frac{a^2}{x} - x \right) \sin\theta \left(S_t - E_o e \left(\frac{a^2}{x} - x \right) \cos\theta \right) T^2 = \frac{1}{8\pi} \left[-\frac{\xi \beta^2 m}{4\pi r} \left(1 - \frac{j}{\beta r} \right) e^{-j\beta r} \cos\theta - \frac{\mu_o \beta^2 m}{4\pi r} \left(1 - \frac{j}{\beta r} - \frac{1}{\beta^2 r^2} \right) e^{-j\beta r} \cos\theta - \frac{\mu_o \beta^2 m}{2\pi r} \left(\frac{j}{\beta r} + \frac{1}{\beta^2 r^2} \right) e^{-j\beta r} \sin\theta \right] \quad (3)$$

$$\frac{\hbar^2}{2m} (\nabla S - eA) e = 0 \quad (4)$$

The importance of the system of equations (1-4) is as follows: (i) it works out the standing waves of equations (1-4) whose solution is of the form

$$T = T(x), \quad S = \omega t, \quad A = 0, \quad e = 1, \quad \theta = f(r, \theta), \quad \omega \in \mathbb{R}$$

(ii) It is useful in evaluating the vital parameters required for the reconfiguration of the transmitting loop antenna. Equations (2) and (4) are somewhat identical within certain constraints. Mathematical analysis using Equation 4 gives the following results

$$\nabla T + (\omega + V_o)^2 T - \left[\omega - E_o e \left(\frac{a^2}{x} - x \right) \cos\theta \right]^2 T - \omega T + 2E_o V_o T - VT = 0 \quad (5a)$$

Equation (5) is referred to as the Euler-Lagrange equation of the function $F: H^1 X D^{1,2} \rightarrow \mathbb{R}$

$$F(T, \theta) = \frac{1}{2} \int_{\mathbb{R}^3} |\nabla U|^2 dx - \frac{(\omega + V_o)}{2} \int_{\mathbb{R}^3} T dx - \frac{\left[\omega - E_o e \left(\frac{a^2}{x} - x \right) \right]}{2} \int_{\mathbb{R}^3} |\cos\theta|^2 dx \quad (5b)$$

Therefore $(T, \theta) \in H^1 X D^{1,2}$ is a critical point of F. The bandwidth of the transmitting antenna is given as

$$B = \frac{\cos\theta}{\pi Q} \left(\frac{\mu_o m}{16\pi r^3 T^2} - E_o^2 \left(\frac{a^2}{x} - x \right) \right) \quad (6)$$

Here Q is the quality factor. The circuitry of a small loop is such that a lumped capacitance C is sometimes placed in parallel with impedance Z to account for the distributed capacitance. Ironically, a loop with uniform current distribution would have no capacitance because no charge exists within the closed loop. The objective in this section is to analyze the possible resonance frequencies in a multi-capacitor small loop circuit when there is uniform current distribution. The theoretical loop design is shown in Figure (2)

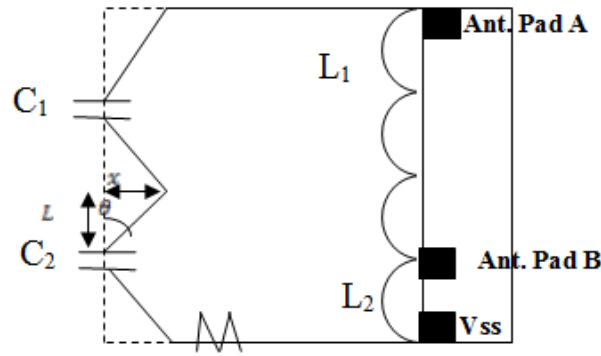


Figure 2. Two Capacitors and Two Inductors Loop-Circuit

The total capacitance of n-number of capacitors is given as

$$C_T(x) = \frac{\text{product } C_n(x)}{\sum_{i=0}^n C_n(x)} \quad (7)$$

In the theoretical design of the loop antenna in Figure (3), the length of the conductor (x) is transformed by applying the Legendre polynomial to calculate the influence of the number of the capacitors when the current distribution in the circuit is uniform.

$$x = 4\pi r \tan\left(\frac{\theta}{2}\right) \quad (8)$$

Alternatively, another technique could be used to understand the effect of the length of the conductor to the current distribution. This technique has been discussed as a derivative of the Maxwell's equation in a quantum mechanical mainframe [4]. Among the functions of the refined Maxwell's postulates (shown in equation 9) is the ability to determine the antenna factor as it relates current distribution.

$$\frac{\partial}{\partial t} E_z = \frac{\partial}{\partial t} E_z e_z e^{-j\beta r} (\sin\theta + \cos\theta) \quad (9)$$

Where α and γ are the attenuation factors of the electrical fields; $E_\gamma(z)$ and $E_\alpha(z)$ are the electric fields generated by the polar difference; β is the frequency of excited power; j is the antenna current; r represents the radius or horizontal component of the antenna; z represents the vertical component of the antenna; m represents the magnitude of the particulates; ξ represents the electrical permeability; μ_0 represents the magnetic permeability; e_r is the spin factor which determines the electron spin along the horizontal component; e_z is the antenna factor which determines the ratio of the electric field strength to the voltage, V is the total potential in space or near earth surface, V_0 is a constant on the surface of the charged air, E_0 is the electric field and a is the antenna potential, x is the Dybe length.

3. Results and Discussion

The advantage of this design is to minimize resistive losses close to 90%. The gain and gain differences were reported to be significantly different from those of regular GPS antenna.

The result is confirmed experimentally in Figure 4 [4-6]. During good weather (see Figure 5), the transmission at 2.4 GHz boost the uplink task (see Figure 4). During rain and fog, the transmission at 24 MHz boost the uplink task (see Figure 4). Hence, the 240 MHz is proposed to boost transmission on the satellite-to-satellite crosslink. Further the incorporation of equation (8) to the simulations in Figures 4 & 5 revealed the possibility of a high efficiency in the transmitting loop antenna via the introduction of angular loop displacement along a well defined axis.

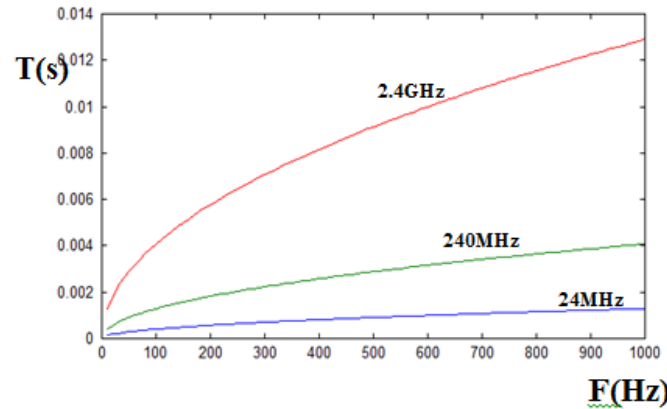


Figure 3. Graph of T against F when F=2.4GHz, 240MHz and 24MHz

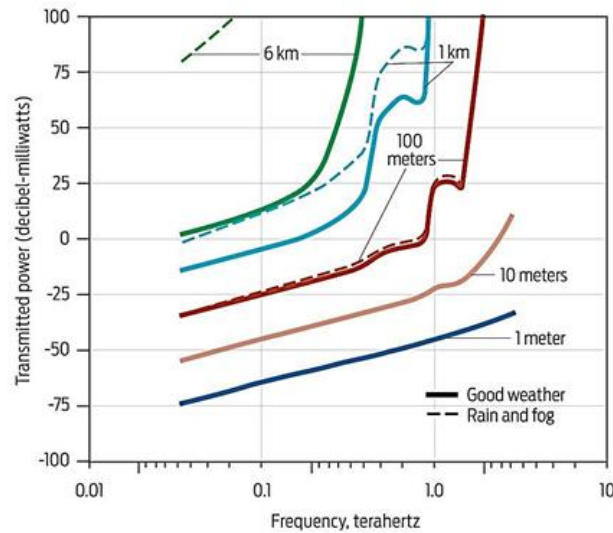


Figure 4, Experimental Confirmation of Figure 3 Ref [5]

The reciprocal of the Antenna factor (AF) is an important to ascertain our previous results on the current distribution. From literature, we expect that the reciprocal of the antenna factor reveals the ratio of the inadequacies of the field strength at the terminal of the antenna. Hence, a negative AF signifies a high electric field strength at the terminal while a positive AF signifies low field strength at the antenna's terminal. In our experimentation via equation (9), we consider an experimentation which enables the sudden change of linearity in Figure. During transmission, weather factors may alter the maximum features of " $\sin\theta + \cos\theta$ " (Figure 5).

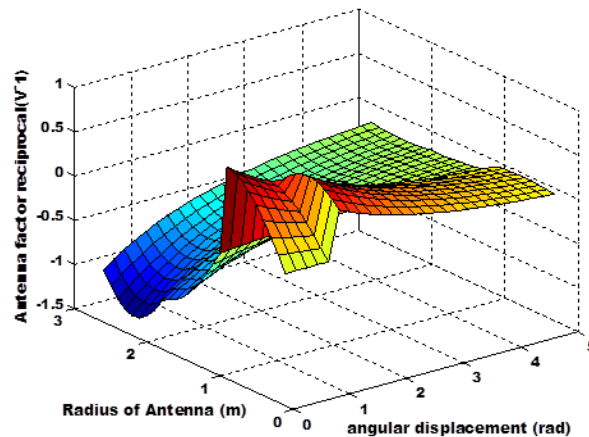


Figure 5. Effect of Antenna Factor Reciprocal on System Performance

The 2D analysis shows that the point where the electric field strength is perfectly equals to the voltage induce is at $\pi/2$. Thus, when the angular loop displacement is $\pi/2$, we expect to see an improved uplink task under either bad or good weather.

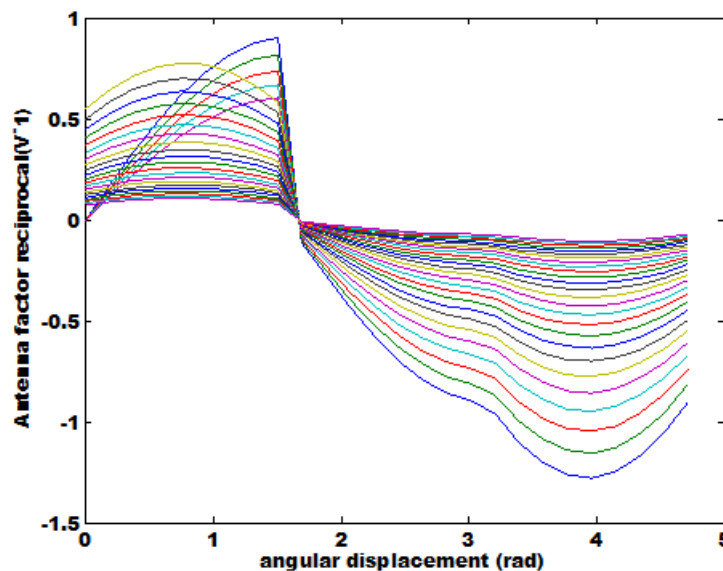


Figure 6. 2D Analysis of Antenna Factor Reciprocal on System Performance

4. Conclusion

The losses in the transmitting loop antenna were analyzed under a theoretical construction whose tuning capacitor is dependent on the length and nature of conductor. Figure (3), reveals the efficiency of the transmitting loop antenna at three different frequencies i.e. 2.4G Hz, 240 MHz and 24 MHz. The function of the standing wave when it ranges from 0 – 1000 m band width allows for possible reconfiguration of the transmitting loop antenna to operate at any of the aforementioned frequencies. Furthermore, the multiple-loop antenna shows good numerical predictions with SMMR between the 100 m and 1km but failure may set in beyond the 1km region. Hence, its principle can be applied to Scanning Multichannel Microwave Radiometer within the acceptable broadband width. When the angular loop displacement is $\pi/2$, we expect to see an improved uplink task under either bad or good weather.

Acknowledgments

The authors acknowledge the sponsorship of Covenant University, Ota, Nigeria.

References

- [1] M. E. Emeter, "Theoretical Modeling Of A Magnetic Loop Antenna for Ultra wideband (UWB) Application", TELKOMNIKA Indonesian Journal of Electrical Engineering, vol. 12, no. 10, (2014), pp. 7076-7081.
- [2] M. E. Emeter, M. L. Akinyemi, U. E. Uno and A. O. Boyo, "Lightning Threat Forecast Simulation Using the Schrodinger-Electrostatic Algorithm", IERI Elsevier Proceeding, vol. 9, (2014), pp. 53-58.
- [3] U. E. Uno and M. E. Emeter, "The Physics Of Remodeling The Transmitting Loop Antenna Using The Schrodinger-Maxwell Equation", Journal for Asian scientific research, vol. 2, no. 1, (2011), pp. 14-24.
- [4] M. E. Emeter, "Investigations of the Sheath Effect on the Resultant Magnetic Field of a Cylindrical Monopole Plasma Antenna", Plasma Science and Technology, vol. 17, no. 2, (2015), pp. 153-158.
- [5] C. M. Armstrong, "The Truth about Terahertz", <http://spectrum.ieee.org/aerospace/military/the-truth-about-terahertz>, (2015).
- [6] J. Goldhirsh, V. Krichevsky and N. E. Gebo, "Rain rate statistics and frequency distributions at 20 and 30 GHz derived from a network of rain gauges in the mid-Atlantic coast over a five-year period", IEEE Trans. Antennas Propagation, vol. 40, no. 11, (1992), pp. 1408-1415.
- [7] W. Schreiner, S. Sokolovskiy, D. Hunt, C. Rocken and Y. H. Kuo, "Analysis of GPS radio occultation data from theFORMOSAT-3/COSMIC and Metop/GRAS missions at CDAAC", Journal of Atmos. Meas. Tech., vol. 4, (2011), pp. 2255-2272.
- [8] J. M. Rasool and M. M. Mool, "Proposed Method of Antenna Array for Receiving Signals from Satellite Mobile Communication", IJCCCE, vol. 14, no. 2, (2014), pp. 1-7.
- [9] C. W. Hearn, "Electrical Design and Testing of an Uplink Antenna for Nanosatellite Applications", M. Sc Thesis, Virginia Polytechnic Institute and State University, (2001), pp. 1-5.
- [10] G. Wübbena, M. Schmitz, G. Mader and F. Czopek, "GPS Block II/IIA Satellite Antenna Testing using the Automated Absolute Field Calibration with Robot", Presented at ION NSS 2007, Sept. 25-28, Fort Worth, Texas, revised version, (2007), pp. 1-8.

Authors



Emeter Moses Eterigho, He currently lectures at Covenant University, Nigeria. His research interest is in theoretical & applied Physics. He has authored two textbooks and over seventy peer reviewed international papers listed on the Thompson Reuters indexed journals, Scopus indexed journals *etc.* He won the prestigious AU/TWAS Young Scientist National Award (Earth and Life Sciences) in 2015. He has won few travel grants to Italy, Malaysia, South Africa, Germany, and Taiwan. Emeter has made salient discoveries in science. Emeter is involved in collaborative research with scientists from Malaysia, Greece and Iran.

